American Journal of Analytical Chemistry, 2016, 7, 57-66
Published Online January 2016 in SciRes. http://www.scirp.org/journal/ajac
http://dx.doi.org/10.4236/ajac.2016.71006

Theoretical and Electrochemical Characterization of δ-$RuCl_2(Nazpy)_2$: Application to Oxidation of D-Glucose

Wawohinlin Patrice Ouattara, Kafoumba Bamba*, Nahossé Ziao, Kouakou Nobel N'guessan

Laboratoire de Thermodynamique et de Physico-Chimie du Milieu, UFR-SFA, Université Nangui-Abrogoua, Abidjan, Côte d'Ivoire
Email: *bambakaf_sfa@una.edu.ci

Received 8 December 2015; accepted 18 January 2016; published 22 January 2016

Abstract

The heterogenized δ-$RuCl_2(Nazpy)_2$ deposited on carbon toray (CT) was studied for the first time as electrochemical catalyst. Before, it was characterized by visible-ultraviolet spectra and theoretically by TDDFT method at B3LYP/Lanl2DZ level. It displayed an MLCT $t_{2g}e_g \rightarrow \pi^*$ transition where $t_{2g}e_g$ due to the structure of Nazpy that considerably reduces energy between d AOs of Ru represents the HOMO of the complex and π^* is identified as the LUMO. Electrochemistry study shows two redox ranges in both negative and positive sides of the potential. The positive side that corresponds to the couple Ru^{IV}/Ru^{III} of catalyst appears to be active for oxidation of D-glucose in carbonate buffer with a high turnover. Therefore, Keto-2-gluconic and gluconic acids were the two main products obtained with respectively 80% and 17.6% of selectivity. Moreover, a small amount of tartaric and glycol acids coming from the c-c bond cleavage due to non-protection of the anomeric carbon of D-glucose were also observed.

Keywords

DFT Calculation, HOMO-LUMO Analysis, NBO, Electrochemistry, Ruthenium Complex, D-Glucose

1. Introduction

Azopyridine dyes have been studied as ligands since recent years. They belong to the π-accepting ligands. They

*Corresponding author.

How to cite this paper: Ouattara, W.P., Bamba, K., Ziao, N. and N'guessan, K.N. (2016) Theoretical and Electrochemical Characterization of δ-$RuCl_2(Nazpy)_2$: Application to Oxidation of D-Glucose. *American Journal of Analytical Chemistry*, **7**, 57-66. http://dx.doi.org/10.4236/ajac.2016.71006

have proven to provide with tremendous results when they are binding metal [1]-[5]. Besides, their performance with ruthenium as complex is more of interest of researchers since ruthenium complex displays a fascinating electron-transfer and energy transfer [6]. Moreover, ruthenium offers a wide range of oxidation states and its reactivities depend on the stability and inter-convertibility of these oxidation states, which in turn depend on the nature of ligands bound to the metal. The fascinating use of azo dyes is that they keep the ruthenium in low states, which increase the complex reactivity and selectivity [7] [8].

In former articles, we showed that azopyridine ligands are assumed to be bidentate [9]. Then, the synthesis that puts together reactive $RuCl_3 \cdot 3H_2O$ and the ligand in methanol gives only two C_2 symmetrical isomers; however the asymmetry of the ligand allows for five isomers [10] [11]. These synthesized isomers are admitted to be γ-Cl and δ-Cl respectively standing for γ-$RuCl_2(L)_2$ and δ-$RuCl_2(L)_2$. L represents azopyridine ligand and the structures of both γ-Cl and δ-Cl mean that both ligands L are respectively in *cis* and *trans* configurations. In this report, we aim to characterize for the first time the $RuCl_2(Nazpy)_2$ where Nazpy stands for 1-(2-pyridilazo)-2-naphtol as electrochemical catalyst for the oxidation of D-glucose and by computer calculation on behalf of DFT method. Regarding its synthesis, previous works reported that the hindrance brought about by Nazpy ligand allowed for the formation of only the isomer δ-$RuCl_2(Nazpy)_2$ [10]. Before, the complex was theoretically supposed to be C_2 symmetrical. Here, although it displays the C_2 axis through Cl-Ru-Cl angle, it is discovered actually to also show a C_i symmetry through Ru that represents the center of symmetry. Therefore, we can assume that δ-Cl is in reality C_i symmetrical. Consequently, both ligands and chloride atoms are identical by pair. Therefore, the investigation will be performed on only δ-$RuCl_2(Nazpy)_2$ isomer. **Figure 1(a)** displays Nazpy ligand showing four hetero-atoms by which the bonding can be performed to ruthenium atom. However, both DFT prediction and experiment show that the most stable complex is obtained when only N_{py} and N_2 are bonded to Ru [12]. Therefore, **Figure 1(b)** displays isomer δ-$RuCl_2(Nazpy)_2$ admitted to be the lone existing complex from reaction between Nazpy and $RuCl_3 \cdot 3H_2O$.

Similar research has been undertaken before, where $RuCl_2(Azpy)_2$ was the regarding complex [13]. Azpy stands for 2-phenylazopyridine. Therein, both isomers γ-Cl and δ-Cl were obviously obtained confirming that the Azpy ligand does not display any steric hindrance. Furthermore, γ-Cl was discovered to be the most active complex since it provides a good yield and important quantity of electricity. Moreover, the main products yielded during electrolysis were assumed to be keto-2-gluconic and gluconic acids. However, with bare platinum as working electrode, only gluconic acid was mainly obtained when D-glucose was oxidized and the active surface was rapidly poisoned.

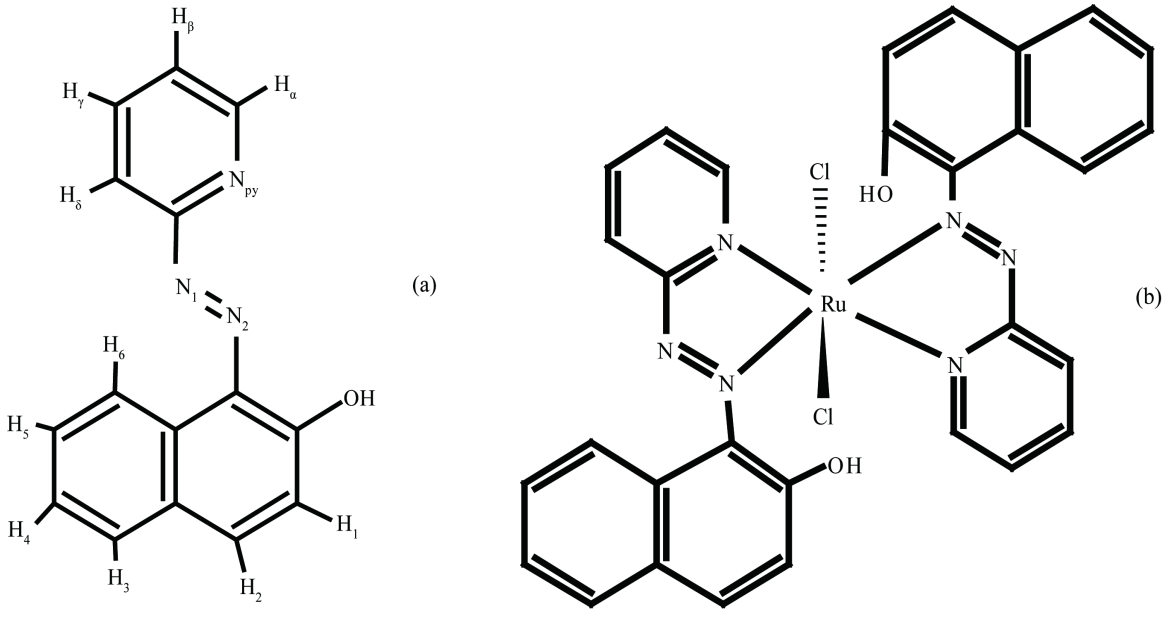

Figure 1. (a) 1-(2-pyridylazo)-2-naphtol(Nazpy) ligand. DFT calculation on ligand shows that the ligand necessarily binds to ruthenium by N_{py} and N_2 forming then a five ring stable shell; (b) δ-$RuCl_2(Nazpy)_2$ indicating both ligands in trans position and both Cl atoms vertically set and opposed.

2. Methods

2.1. Materials

All the reagents were used as received. 1-(2-pyridylazo)-2-naphtol was bought from AVOCADO, $RuCl_3 \cdot 3H_2O$ was thanks to Alfa Aeser from Johnson Mathey Company. Organics products were from Fluka, Merck and Sigma. $RuCl_2(Nazpy)_2$ was synthesized by using published procedure [3].

2.1.1. Experiment Measurement

Electronic spectra were recorded with an ultroscan LKB (4050/4051) in DMSO solvent. Electrochemical measurements (cyclic voltammetric, controlled potential-coulometry) were made thanks to a merger of: PC computer (commodore), a potentiostat generator (EG & G, model 362), a coulometer (wenking EVI 80, bank electronic) and a recorder (Kipp & Zonen, BD 90).Three electrodes that were used comprise:

- The working electrode is formed with an alloy of palladium-gold wire and a carbon toray (CT). The powder of the catalyst δ-$RuCl_2(Nazpy)_2$ is deposited on CT after its mixture in a merger nafion-water (80 mL/80mL). 14.4 mg of the powder was deposited on CT surface that geometric area is $s = 4.5$ cm^2).
- The auxiliary electrode is a vitreous carbonic.
- The reference electrode is a reversible mercuric sulfate (MSE).

Before each experiment, the solution was bubbled with a stream of nitrogen gas (U quality from Air liquid) to get rid of oxygen and then the gas was maintained over the solution during measurements to keep it off oxygen.

Electrolysis was undertaken in a double compartments cell to separate both working and auxiliary electrodes so that we could avoid reducing oxidized compounds [14]. The electrolyzed products were identified by ionic chromatography (HPIC 4500i from Dionex).

2.1.2. Computational Methods

All calculations were performed on the optimized geometry of the complex. The optimized geometry and all other calculations were undertaken at B3LYP/LANL2DZ level. LANL2DZ basis set is known to be an effective core potential (ECP) which is admitted to display accurate results with transition metals [15]. Besides, it is also suitable for any atom. NMR prediction was carried out at B3LYP/LANL2DZ level with GIAO method to confirm the C_i symmetry of δ-Cl. Furthermore, TD-DFT and NBO calculations were performed to figure out the electronic transition modes. Before, frequency calculation was performed on optimized molecule to find out the minima of Potential-Energy-Surface (PES) that characterizes the stable state of molecules. All the calculations were performed using Gaussian 03 program package [16].

3. Results and Discussions

3.1. NMR Calculation of γ- and δ-$RuCl_2(Nazpy)_2$

Figure 1(a) shows the Nazpy ligand that owns all the hydrogen atoms within the complex. Therefore, **Table 1** displays the ^{1}H NMR recorded by theory and experiment of both isomers. The prediction was performed at B3LYP/Lanl2dz level both for the ligand and the isomers.

Through **Table 1**, it can be seen that δ-$RuCl_2(Nazpy)_2$ displays chemical shifts that match well with the experimental data. The most deshielded protons are assumed to be H_α, H_δ and H_6. Therefore, as confirmed by H NMR that $RuCl_2(Nazpy)_2$ synthesized is δ-Cl certainly due to the hindrance of Nazpy, we can admit that it is a C_i symmetrical. Consequently, the upcoming works will be performed only on δ-$RuCl_2(Nazpy)_2$ isomer.

3.2. Characterization of δ-$RuCl_2(Nazpy)_2$

Besides the NMR characterization of δ-$RuCl_2(Nazpy)_2$ that confirms its C_i symmetry, the electronic data was studied and the spectra recorded are displayed in **Figure 2** and in **Table 2**. It shows the maximum wavelength recorded by experiment and theory in DMSO on both Nazpy ligand and δ-$RuCl_2(Nazpy)_2$. It follows that the main data recorded by experiment is $\lambda = 590$ nm. It must correspond to $t_{2g}(Ru) \rightarrow \pi^*$ (L) known as Metal to Ligand Charge Transfer (MLCT) transition. Moreover, the remaining three data are assumed to come from transition within ligand. Thus, the values that are $\lambda = 290$, 400 and 468 nm match well with the dashed spectrum that corresponds to ligand Nazpy characterized in the same condition. The spectra are accepted to be respectively $n \rightarrow \sigma^*$, $n \rightarrow \pi^*$ and $\pi \rightarrow \pi^*$ or Ligand to Ligand Charge Transfer (LLCT) transitions [17].

Table 1. ^{1}H NMR calculated at B3LYP/Lanl2dz level of both γ-Cl and δ-Cl isomers and ligand compared with experiment values. Both γ-Cl and δ-Cl are respectively C_2 and C_i symmetrical.

	Theoretical data at B3LYP/Lanl2dz			Experimental [12] data in $CDCl_3$	
	Ligand	γ-Cl	δ-Cl	Ligand	$RuCl_2(Nazpy)_2$
H_α	9.23	9.91	9.59	8.41	8.87
H_β	7.66	8.07	7.76	7.12	7.72
H_γ	8.26	8.67	8.50	7.81	8.43
H_δ	8.41	8.84	8.91	7.88	8.44
H_1	6.86	6.66	7.94	6.70	7.11
H_2	7.88	7.77	8.27	7.64	8.32
H_3	7.72	7.83	8.03	7.92	8.08
H_4	7.67	7.84	7.87	7.40	8.01
H_5	8.00	7.89	7.89	7.52	7.90
H_6	9.62	8.60	8.72	8.41	8.85

Table 2. Second order perturbation highlighting relation between electronic transition and UV visible data. Theoretical values were determined at B3LYP/LANL2DZ with TDDFT method in DMSO phase.

Character	Donor→ Acceptor		Experimental data λ (nm)		Theoretical data λ (nm)	
	Ligand (Nazpy)	δ-$RuCl_2(Nazpy)_2$	Ligand	δ-$RuCl_2(Nazpy)_2$	Ligand	δ-$RuCl_2(Nazpy)_2$
LLCT	$LP(N_{py}) \rightarrow \sigma^*(C\text{-}C)$	$LP(N_1) \rightarrow \sigma^*(N_{py}\text{-}C)$	290	290	293	
LLCT	$LP(O) \rightarrow \pi^*(C\text{-}C)$	$LP(O) \rightarrow \pi^*(C\text{-}C)$	400	400	393	371
LLCT	$\pi(C\text{-}C) \rightarrow \pi^*(C\text{-}C)$	$\pi(C\text{-}C) \rightarrow \pi^*(C\text{-}C)$	468	468	596	607
MLTC		$LP(Ru) \rightarrow \pi^*(N_1\text{-}N_2)$		590		689

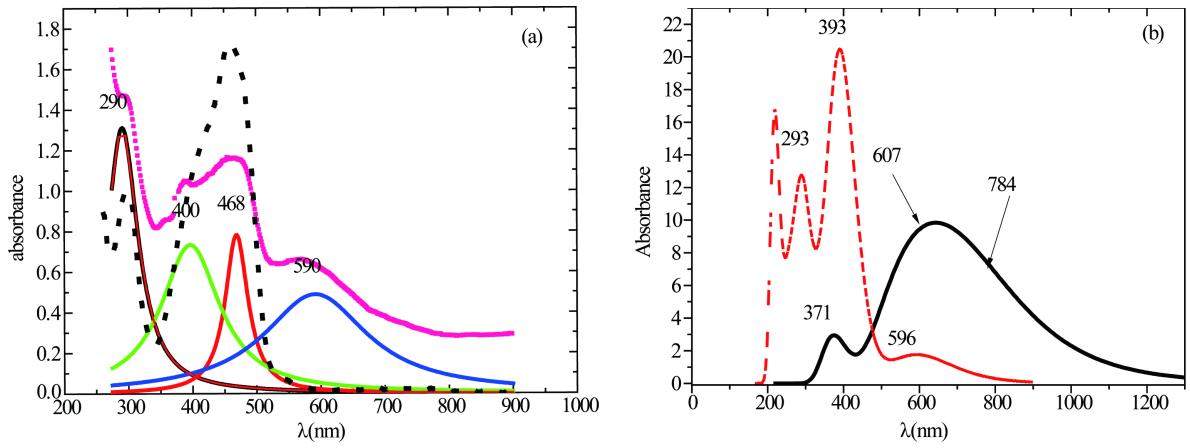

Figure 2. Electronic spectra of $RuCl_2(Nazpy)_2$ and ligand Nazpy (a) recorded in DMSO solvent, solid lines represent $RuCl_2(Nazpy)_2$ and dot line characterizes the ligand; (b) Electronic data predicted at B3LYP/LANL2DZ level with TDDFT method in DMSO phase. Here, dash line characterizes the ligand and solid line deals with the complex's spectrum.

Figure 2(b) displays the theoretical investigation performed on both ligand and δ-$RuCl_2(Nazpy)_2$ in DMSO phase at B3LYP/Lanl2dz level. Regarding the ligand, it shows three bands and their wavelengths are λ = 293, 393 and 596 nm. The high value of 596 nm from the experimental value (λ = 468 nm) can be due to the solvent

used for calculation. Concerning δ-$RuCl_2(Nazpy)_2$, it shows a first band at λ = 371 nm. The second band is large and includes a shoulder at λ = 607 and a main band at λ = 784 nm that must be the MLCT $t_2(Ru) \rightarrow \pi^*(L)$ transition. Whereas the bands at 371 and at 607 nm, they are assumed to match with transitions within the ligand Nazpy. Anyway, we can see a real shift between both experimental and theoretical data certainly due the solvent integrated in prediction. To well understand these transitions, NBO calculation was carried out. Therefore, the second-order perturbation highlighting donor-acceptor (bond-antibond) interactions exhibits the interaction $LP(Ru) \rightarrow *(N_1\text{-}N_2)$ that bears out the MLCT transition. **Table 2** summarizes all possible transitions within both the ligand and δ-$RuCl_2(Nazpy)_2$.

Table 2 shows that oxygen is involved in the interaction within both ligand and the complex according to transition $LP(O) \rightarrow \pi^*(C\text{-}C)$. Moreover, the donor of electron through the transition regarding $n \rightarrow \sigma^*$ can probably be explained by the value of occupancy and the availability of N atom. In the complex, as N_{py} is involved in the bonding Ru-N_{py}, it shares its occupancies with Ru atom instead of performing transition $n \rightarrow \sigma^*$. Therefore, only N_1 whose value of occupancy is 1.94 should necessarily be concerned by the transition $n \rightarrow \sigma^*$ in the complex. Besides, when analyzing the HOMO-LUMO orbitals, it follows that LP(Ru) corresponds to HOMO orbital and its natural hybrid structure is $h_{Ru} = 0.46(4d_{xy}) + 0.53(4d_{xz}) + 0.20(4d_{yz}) - 0.63\left(4d_{x^2-y^2}\right) + 0.26\left(4d_{z^2}\right)$. It shows that HOMO is made of t_{2g} orbitals that include d_{xy}, d_{xz} and d_{yz} atomic orbitals. However, the hybrid also comprises two others AOs that correspond to e_g MO. Therefore, that particularity of the hybrid h_{Ru} structure where both t_{2g} and e_g MOs form the same cloud of electrons can be explained by the closeness of the energies of the five atomic d orbitals (AOs) of the metal as highlights **Table 3**. It shows that all AOs in the complex have almost the same energy and therefore, they must all be involved in the hybridization. In the contrary, Ru atom displays AOs whose energy are actually different and the occupancies are distributed according to energy values indicates a significant discrepancy between t_{2g} and e_g orbitals. Thus, we can assume that the ligand Nazpy induces a weak field [18]. Otherwise, the stabilization energy of the ligands field is assumed to be shallow allowing all the five AOs to share the d electrons **7.16** occupancies as indicates the electron configuration of Ru according to NBO analysis: [core]5s(0.27)4d(7.16)5p(0.01)5d(0.03)6p(0.02).

Therefore, we can conclude anyway that the HOMO is exclusively made of metallic orbital d of the ruthenium. So the electronic transition must be written as $\mathbf{t_{2g}e_g(Ru) \rightarrow \pi^*(N_1 - N_2)}$. Regarding LUMO orbital, it corresponds to $\pi^*(N_1 - N_2)$ which natural hybrid structure for N_2 atom is $h_N = 0.99(2p_x) - 0.12(2p_y)$ and the overlap of both atomic obitals (AOs) that confirms the p character of the molecular orbital is written as follow: $\pi^*_{N_2-N_1} = 0.68\left(p(99.99\%)\right)_{N_2} - 0.73\left(p(99.99\%)\right)_{N_1}$.

3.3. Electrochemical Characterization

Cyclic voltammetry is assumed to be the most versatile electroanalytical technique for the study of species. It permits to rapidly observe redox behavior over a wide range of potential [19]. **Figure 3** displays two voltammograms of δ-$RuCl_2(Nazpy)_2$ recorded in carbonate buffer (0,1 M $Na_2CO_3/NaHCO_3$).

The voltammogram of **Figure 3(a)** has been recorded in the negative range of the potential from −950 mV to −450 mV/MSE. During the positive sweep, an oxidative peak can be observed at −486 mV/MSE. Regarding the reductive peak, it is observed at −616 mV/MSE during the negative sweep of the rate. Therefore, The peak-to-peak ΔE = 130 mV shows that the system is quasi-reversible and it is assigned to the couple Ru(III)/Ru(II). The second voltammogram regarding **Figure 3(b)** is attributed to the couple Ru(IV)/Ru(III). Herein, the positive sweep of the rate indicates an oxidation peak at 323 mV/MSE corresponding to Equation (1).

$$RuCl_2\left(Nazpy\right)_2^+ \rightarrow RuCl_2\left(Nazpy\right)_2^{2+} + e^- \quad (1)$$

Table 3. Populations and energy (a.u.) of d AOs of both Ru atom and Ru in δ-$RuCl_2(Nazpy)_2$.

Ru (in)	d_{xy}		d_{yz}		d_{xz}		$d_{x^2-y^2}$		d_{z^2}	
	Population	Energy	Population	Energy	Population	Energy	Population	Energy	Population	Energy
δ-Cl	1.48	−0.22	1.63	−0.22	1.56	−0.23	1.29	−0.21	1.20	−0.2
atom	2	−0.2	2	−0.18	2	−0.18	0	−1	1.5	−0.15

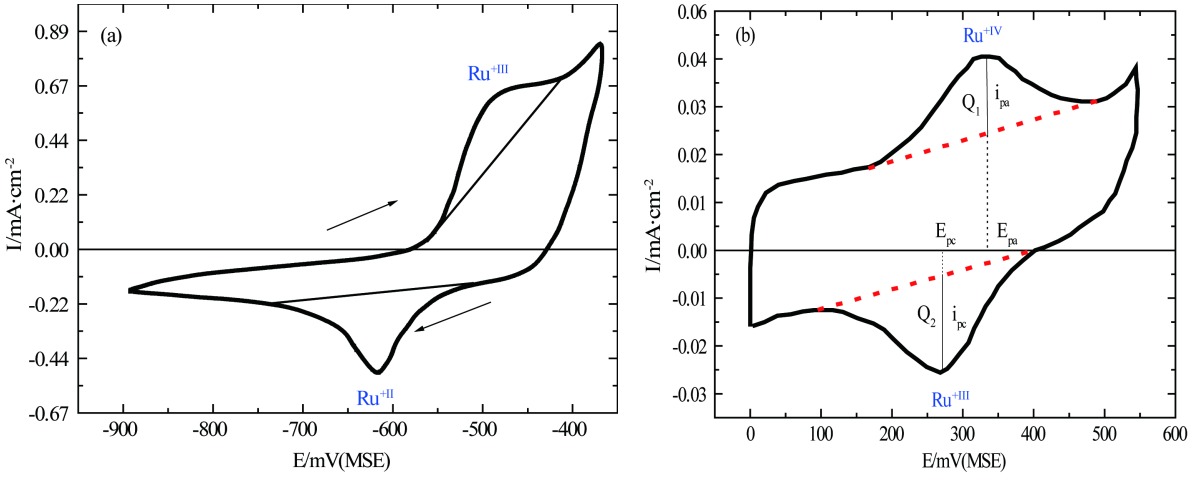

Figure 3. Cyclic voltammogram of δ-$RuCl_2(Nazpy)_2$/nafion-water-C_t in $NaHCO_3/Na_2CO_3$ 0,1 M at a scan rate of 50 mV/S and at 298.15 K: (a) Potential range regards Ru^{III}/Ru^{II}; (b) Potential range concerns Ru^{IV}/Ru^{III}. i_{pa} and i_{pc} stands respectively for anodic and cathodic peaks currents.

Besides, the reductive peak recorded during the reverse sweep of the rate is at 277 mV/MSE and the regarding reaction is characterized by Equation (2).

$$RuCl_2\left(Nazpy\right)_2^{2+} + e^- \rightarrow RuCl_2\left(Nazpy\right)_2^{+} \tag{2}$$

Therefore, the peak-to-peak separation ΔE = 46 mV/MSE indicates a reversible system and this reversibility was borne out by the ratio peaks currents

$$\frac{i_{pa}}{i_{pc}} = \frac{0.016}{0.019} \approx 1. \tag{3}$$

Moreover, the number of electrons transferred in the electrode reaction for the couple is obtained by Equation (4).

$$\Delta E = E_{pa} - E_{pc} = \frac{0.059}{n} \tag{4}$$

It follows that both systems are consistent with the literature since it has been assumed that electron exchange comes exclusively from ruthenium atom. Thus, the ligands are merely concerned by rendering the Ru atom more selective [8]. Moreover, electrochemical characterization of $RuCl_3 \cdot 3H_2O$ performed in previous paper shows well the difference between both catalysts [13]. This discrepancy is due to ligand lowering the redox values in the complex. Furthermore, we calculated the quantity of electricity by integration of the surfaces of both positive and negative peaks of the latter voltammogram though the potential range fits well with oxidation potential of carbohydrate molecules. Therefore, as indicated in **Figure 3(b)**, Q_1 and Q_2 are equal confirming the reversible state of the system. So, the quantity of electricity calculated was as well for the oxidation as for the reduction surfaces Q = 263 µC.

3.4. Electrolysis Study of D-Glucose

D-glucose was oxidized over a working electrode δ-$RuCl_2(Nazpy)_2$/CT. The reaction last out 48 h. Before, **Figure 4** displays voltammogram recorded over 50 $mmol \cdot L^{-1}$ of D-glucose compared with that recorded in supporting electrolyte alone. In presence of D-glucose, a reductive peak was absent confirming the fast reaction between Ru^{IV} and the sample. This voltammogram was recorded at the beginning of the electrolysis to find out the best potential to be fixed up for oxidation of D-glucose. Therefore, the accepted potential which current was the most important was 600 mV/MSE. In consequence, the prolonged electrolysis was then performed by setting the electrolysis potential at 600 mV/MSE to renew the oxidation state of Ru.

The density current observed at the beginning was j = 49 $\mu A \cdot mg^{-1}$. This value decreased during 15 hours and

stabilized at j = 16 μA·mg^{-1}. At the end, the current was however 14 μA·mg^{-1} and the quantity of electricity was 45.1C with a yield of 20.5% of D-glucose. **Figure 5** presents the evolution of both quantity of current and the density of electricity recorded during the prolonged electrolysis.

Furthermore, the electrolyzed products were analyzed thanks to ionic chromatography. Herein, new more products were obtained that have never been yielded since the recognized most active catalysts as platinum and gold were used [20]-[23]. Keto-2-gluconic and gluconic acids were obtained respectively with 80% and 17.6% of selectivity. Besides, small amounts of products like tartaric and oxalic acids coming from C-C cleavage were also observed. The particularity of the catalyst is that it has been used for many times, and it did not suffer from any damage. **Figure 6** summarizes the evolution of transformation of D-glucose into the main products aforementioned.

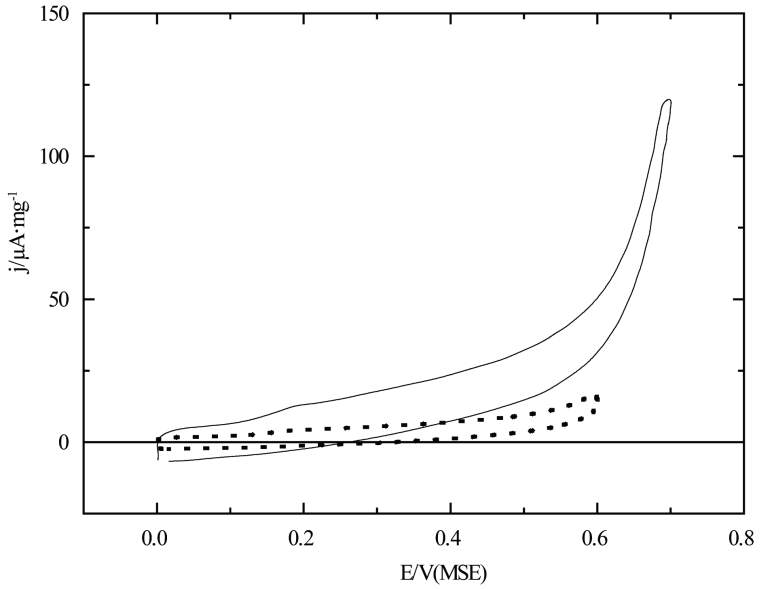

Figure 4. Voltammograms of δ-$RuCl_2(Nazpy)_2$/CT recorded in $NaHCO_3$-Na_2CO_3 0.1 mol·L^{-1}, at 50 mV·s^{-1} and at 25˚C. (---) supporting electrolyte alone; (—) in presence of 50 mmol·L^{-1} of D-glucose.

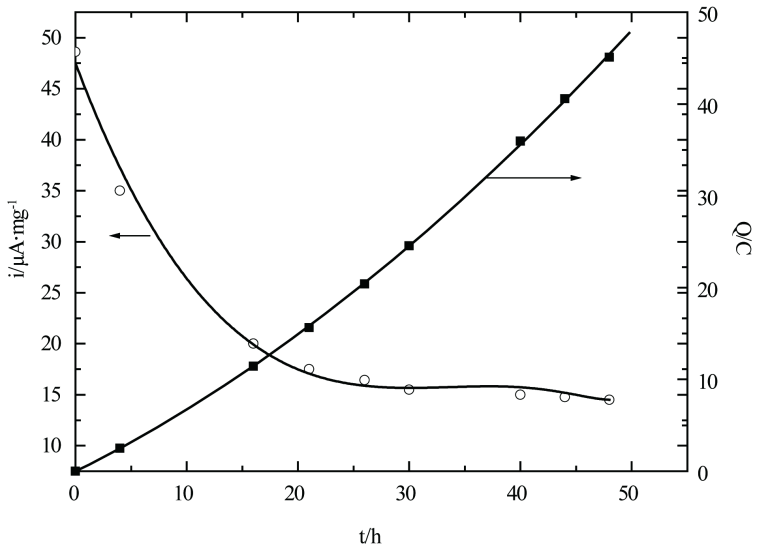

Figure 5. Evolution of current density (○) and quantity of electricity (■) versus time during the electrolysis of D-glucose over δ-$RuCl_2(Nazpy)_2$/CT.

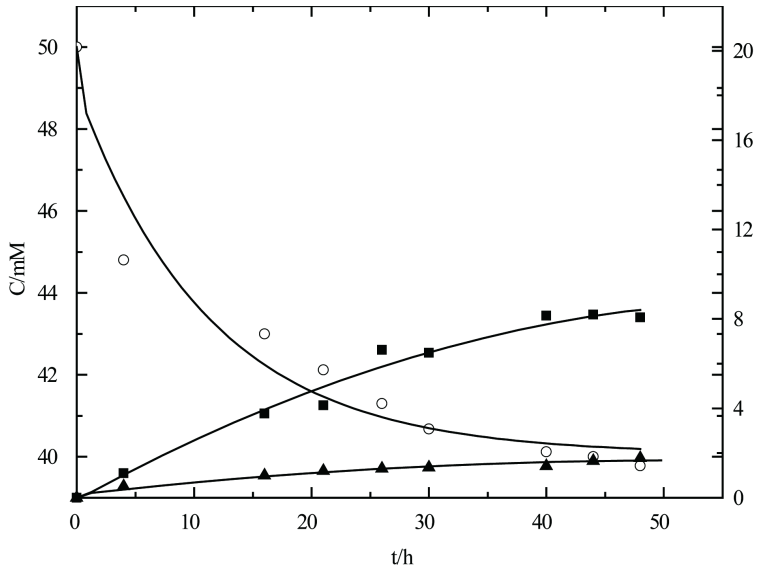

Figure 6. Evolution of concentrations of D-glucose (○) and the main products during prolonged electrolysis over δ-$RuCl_2(nazpy)_2$. (■) keto-2-gluconic acid, (▲) gluconic acid.

4. Conclusions

C_i symmetrical δ-$RuCl_2(Nazpy)_2$ was studied for the first time as working electrode for oxidation of D-glucose. Before, its characterization by UV visible technique and TDDFT method at B3LYP/LANL2DZ level was carried out in DMSO phase. A MLCT and three LLCT transitions were obtained. The MLCT is assumed to be $t_{2g}e_g \rightarrow \pi^*$ transition, though the HOMO is a linear combination of the five atomic d orbitals as their energies are very close. The regarding hybridization according to NBO analysis is: $h_{Ru} = 0.46(4d_{xy}) + 0.53(4d_{xz}) + 0.20(4d_{yz}) - 0.63\left(4d_{x^2-y^2}\right) + 0.26\left(4d_{z^2}\right)$. Nazpy is therefore assumed to reduce energy gap between the five AOs d of Ru on the benefit of the well sharing electrons.

Besides, cyclic voltammetry performed on the heterogeneous catalyst displayed two redox couples. The first couple that was discovered in negative range of potential was Ru^{+III}/Ru^{+II}. This process was irreversible though the peak-to-peak separated potential was ΔE = 130 mV/MSE. The second range was recorded in positive range of the potential between 0 and 600 mV/MSE. The peak-to-peak separated potential ΔE = 46 mV indicated a reversible system, and the regarding redox couple was assumed to be Ru^{+IV}/Ru^{+III}. The electro-oxidation of D-glucose was undertaken at 600 mV/MSE as this potential was the convenient one to renew the Ru^{+IV} state. Therefore, keto-2-gluconic and gluconic acids were both the main products yielded with respectively 80% and 17.6% amounts of selectivity. These products were the same obtained when $RuCl_2(Azpy)_2$ was studied as mediators where the current produced was unfortunately feeble. Comparatively to platinum that is up to now recognized to be the best active catalyst, however its active sites are rapidly poisoned; the azopyridine complex of ruthenium is assumed to be more selective.

References

[1] Krause, R. and Krause, K. (1982) Chemistry of Bipyridyl Like Ligands. 2. Mixed Complexes of Ruthenium(II) with 2-(Phenylazo)pyridine: A New .pi.-Bonding Probe. *Inorganic Chemistry*, **21**, 1714-1720. http://dx.doi.org/10.1021/ic00135a002

[2] Krause, R. and Krause, K. (1980) Chemistry of Bipyridyl-Like Ligands. Isomeric Complexes of Ruthenium(II) with 2-(Phenylazo)pyridine. *Inorganic Chemistry*, **19**, 2600-2603. http://dx.doi.org/10.1021/ic50211a024

[3] Goswami, S., Chakravarty, A.R. and Chakravorty, A. (1981) Chemistry of Ruthenium. 2. Synthesis, Structure, and Redox Properties of 2-(Arylazo)pyridine Complexes. *Inorganic Chemistry*, **20**, 2246-2250. http://dx.doi.org/10.1021/ic50221a061

[4] Goswami, S., Chakravarty, A.R. and Chakravorty, A. (1982) Chemistry of Ruthenium. 5. Reaction of Trans-dihalobis [2-(arylazo)pyridine]ruthenium(II) with Tertiary Phosphines: Chemical, Spectroelectrochemical, and Mechanistic

Characterization of Geometrically Isomerized Substitution Products. *Inorganic Chemistry*, **21**, 2737-2742. http://dx.doi.org/10.1021/ic00137a040

[5] Goswami, S., Chakravarty, A.R. and Chakravorty, A. (1983) Chemistry of Ruthenium. 7. Aqua Complexes of Isomeric Bis[(2-arylazo)pyridine]ruthenium(II) Moieties and Their Reactions: Solvolysis, Protic Equilibriums, and Electrochemistry. *Inorganic Chemistry*, **22**, 602-609. http://dx.doi.org/10.1021/ic00146a007

[6] Heeres, A., van Doren, H.A., Gotlieb, K.F. and Bleeker, I.P. (1997) Synthesis of α- and β-d-Glucopyranuronate 1-Phosphate and α-d-Glucopyranuronate 1-Fluoride: Intermediates in the Synthesis of d-Glucuronic Acid from Starch. *Carbohydrate Research*, **299**, 221-227. http://dx.doi.org/10.1016/S0008-6215(97)00030-X

[7] Basuli, F., Das, A.K., Mostafa, G., Peng, S.-M. and Bhattacharya, S. (2000) Chemistry of Ruthenium with Some Phenolic Ligands: Synthesis, Structure and Redox Properties. *Polyhedron*, **19**, 1663-1672. http://dx.doi.org/10.1016/S0277-5387(00)00404-6

[8] Boelrijk, A.E.M., Anja, M., Jorna, J. and Reedijk, J. (1995) Oxidation of Octylα-d-glucopyranoside to Octylα-d- glucuronic Acid, Catalyzed by Several Ruthenium Complexes, Containing a 2-(Phenyl)azopyridine or a 2-(Nitrophenyl) azopyridine Ligand. *Journal of Molecular Catalysis A*: *Chemical*, **103**, 73-85. http://dx.doi.org/10.1016/S0277-5387(00)00404-6

[9] Affi, S.T., Bamba, K. and Ziao, N. (2015) Computational Characterization of Organometallic Ligands Coordinating Metal: Case of Azopyridine Ligands. *Journal of Theoretical and Computational Chemistry*, **14**, Article ID: 1550006. http://dx.doi.org/10.1142/s0219633615500066

[10] N'Guessan, K.N., Bamba, K., Ziao, N. and Ouattara, W.P. (2015) Molecular Structure, Vibrational Spectra and NMR Analyses on Two Azopyridine Ruthenium Complexes Using Density Functional Theory Calculations. *Journal of Chemical and Pharmaceutical Research*, **7**, 246-252.

[11] Velders, A.H., Van der Schilden, K., Hoste, A.C.G., Reedijk, J., Kooijman, H. and Speck, A.L. (2004) Dichlorobis(2-phenylazopyridine)ruthenium(II) Complexes: Characterization, Spectroscopic and Structural Properties of Four Isomers. *Dalton Transactions*, **3**, 448-455. http://dx.doi.org/10.1039/b313182c

[12] Bamba, K. (2004) Oxydation électrocatalytique de monosaccharides sur des complexes de ruthénium et sur le platine modifié par des adatomes métalliques. PhD Thesis, University of Poitiers, Poitiers, 70.

[13] Bamba, K., Leger, J.-M., Garnier, E., Bachmann, C., Servat, K. and Kokoh, K.B. (2005) Selective Electro-Oxidation of D-Glucose by $RuCl_2(azpy)_2$ Complexes as Electrochemical Mediators. *Electrochimica Acta*, **50**, 3341-3346. http://dx.doi.org/10.1016/j.electacta.2004.12.007

[14] Greef, R., Peat, R., Peter, L.M., Pletcher, D. and Robinson, J. (1985) Instrumental Methods Electrochemistry, the Design of Electrochemical Experiments. Ellis Horwood Limited, Southampton Electrochemistry Group, 359.

[15] Chen, J.C., Li, J., Qian, L. and Zheng, K.C. (2005) Electronic Structures and SARs of the Isomeric Complexes α-, β-, γ-$[Ru(mazpy)_2Cl_2]$ with Different Antitumor Activities. *Journal of Molecular Structure*: *THEOCHEM*, **728**, 93-101. http://dx.doi.org/10.1016/j.theochem.2005.05.005

[16] Frisch, M.J., Trucks, G.W., Schlegel, H.B., Scuseria, G.E., Robb, M.A., Cheeseman, J.R., Montgomery, Jr., J.A., Vreven, T., Kudin, K.N., Burant, J.C., Millam, J.M., Iyengar, S.S., Tomasi, J., Barone, V., Mennucci, B., Cossi, M., Scalmani, G., Rega, N., Petersson, G.A., Nakatsuji, H., Hada, M., Ehara, M., Toyota, K., Fukuda, R., Hasegawa, J., Ishida, M., Nakajima, T., Honda, Y., Kitao, O., Nakai, H., Klene, M., Li, X., Knox, J.E., Hratchian, H.P., Cross, J.B., Adamo, C., Jaramillo, J., Gomperts, R., Stratmann, R.E., Yazyev, O., Austin, A.J., Cammi, R., Pomelli, C., Ochterski, J.W., Ayala, P.Y., Morokuma, K., Voth, G.A., Salvador, P., Dannenberg, J.J., Zakrzewski, V.G., Dapprich, S., Daniels, A.D., Strain, M.C., Farkas, O., Malick, D.K., Rabuck, A.D., Raghavachari, K., Foresman, J.B., Ortiz, J.V., Cui, Q., Baboul, A.G., Clifford, S., Cioslowski, J., Stefanov, B.B., Liu, G., Liashenko, A., Piskorz, P., Komaromi, I., Martin, R.L., Fox, D.J., Keith, T., Al-Laham, M.A., Peng, C.Y., Nanayakkara, A., Challacombe, M., Gill, P.M.W., Johnson, B., Chen, W., Wong, M.W., Gonzalez, C. and Pople, J.A. (2003) Gaussian 03's Program. Gaussian, Inc., Pittsburgh, PA. http://gaussian.com/

[17] Kalia, K.C. and Chakravorty, A. (1970) Hydrogen Bonding and Isomerism in Arylazooximes. *Journal of Organic Chemistry*, **35**, 2231-2234. http://dx.doi.org/10.1021/jo00832a027

[18] Shriver, D.F. and Atkins, P.W. (1999) Inorganic Chemistry. 3rd Edition, Oxford University Press, Oxford, 230.

[19] Sawyer, D.T., Heineman W.R. and Beebe, J.M. (1984) Chemistry Experiments for Instrumental Methods. John Wiley and Sons, New York, 79.

[20] Kokoh, K.B. (1991) Oxydation régiosélective du d-glucose par voie électrocatalytique. Thèse de doctorat, Université de Poitiers, Poitiers.

[21] Essis-Yei, L.H. (1987) Oxydation electrocatalytique du glucose sur le platine et l'or en milieu aqueux. Thèse de Doctorat, Université de Poitiers, Poitiers.

[22] Bamba, K., Kokoh, K.B., Servat, K. and Léger, J.-M. (2006) Electrocatalytic Oxidation of Monosaccharides on Plati-

num Electrodes Modified by Thallium Adatoms in Carbonate Buffered Medium. *Journal of Applied Electro-Chemistry*, **26**, 233-238. http://dx.doi.org/10.1007/s10800-005-9056-0

[23] Beden, B., Leger, J.-M. and Lamy, C. (1992) Electrocatalytic Oxidation of Oxygenated Aliphatic Organic Compounds at Noble Metal Electrods. *Modern Aspects of Electrochemistry*, **22**, 97-264.